JACS
JOURNAL OF THE AMERICAN CHEMICAL SOCIETY
Communication
pubs.acs.org/JACS

Ab Initio Time-Domain Study of the Triplet State in a Semiconducting Carbon Nanotube: Intersystem Crossing, Phosphorescence Time, and Line Width

Bradley F. Habenicht[†] and Oleg V. Prezhdo*[,‡]

[†]Center for Nanophase Materials Sciences, Oak Ridge National Laboratory, Oak Ridge, Tennessee 37830, United States
[‡]Department of Chemistry, University of Rochester, Rochester, New York 14627, United States

Supporting Information

ABSTRACT: Motivated by recent experiments (*J. Am. Chem. Soc.* **2011**, *133*, 17156), we used nonadiabatic (NA) molecular dynamics implemented within ab initio time-domain density functional theory to investigate the evolution of the excited electronic singlet and triplet states in the (6,4) carbon nanotube (CNT). The simulation simultaneously included the NA electron−phonon interaction and the spin−orbit (SO) interaction and focused on the intersystem crossing (ISC) from the first excited singlet state (S_1) to the triplet state (T_1) and subsequent relaxation to the ground electronic state (S_0). For the first time, the state-of-the-art methodology (*Phys. Rev. Lett.* **2005**, *95*, 163001; *Phys. Rev. Lett.* **2008**, *100*, 197402) has been advanced to include triplet states. The S_1−T_1 ISC was calculated to occur within tens of picoseconds, in agreement with the experimental data. This time scale is on the same order as the S_1−S_0 nonradiative decay time obtained previously for the (6,4) CNT. The homogeneous phosphorescence line width, which can be measured in single-molecule experiments, was predicted to be on the order of 10 meV at room temperature. This value is similar to the fluorescence line widths of CNTs suspended in air. The NA electron−phonon and SO couplings were found to be on the order of 1 meV; however, the former fluctuates much more than the latter, causing the ISC rate to be limited by the SO interaction rather than NA interaction. The electronic energy lost nonradiatively during ISC is deposited into high-frequency optical phonons of the CNT arising from C−C stretching motions. The calculations indicate that ISC can contribute to the nonradiative energy losses and low photoluminescence quantum yields observed in semiconducting CNTs.

The photophysics of carbon nanotubes (CNTs) has received great attention over the past decade.[1,2] Significant progress has been made in understanding the fundamental nature of the electronic excitations in CNTs[3,4] and the corresponding channels for energy dissipation.[5−9] Still, great uncertainties remain, particularly in the lifetimes of the excited electronic states of CNTs. Experimental reports vary over several orders of magnitude, ranging from picoseconds to nano- and microseconds.[5,9−11] Theoretical estimates of the radiative lifetimes are on the nanosecond time scale,[12,13] while the nonradiative relaxation has been evaluated to occur within hundreds of picoseconds in perfect CNTs and tens of picoseconds in CNTs with defects.[6,7] The observed low quantum yields of photoluminescence (PL)[14−16] present a great practical difficulty in numerous CNT applications.[17−21] Experimental studies have concluded that nonradiative decay mechanisms dominate the relaxation of both bound excitons and free charge carriers in CNTs.[5,9−11] The excitonic splitting into bright and dark singlet states, as well as the presence of triplets, complicates the issue further.[5,22,23] Static electronic structure calculations using high-level ab initio density functional theory (DFT)[24,25] and semiempirical Hamiltonians[26,27] have provided estimated singlet and triplet energies and splittings. Time-domain theoretical studies of the relaxation pathways constitute the next step in elucidating and consolidating the conflicting experimental evidence. Recently, the dynamics of intersystem crossing (ISC) into and out of the lowest-energy triplet excited state of a single-walled CNT has been characterized experimentally in the time domain,[5] motivating the current theoretical work.

Here we present the first ab initio time-domain simulation of ISC between singlet and triplet electronic states in a CNT. We considered optical line widths and nonradiative relaxation times for the transitions from the lowest-energy excited singlet state (S_1) to the lowest triplet state (T_1) and from T_1 to the ground state (S_0) (Figure 1). The study was made possible by the

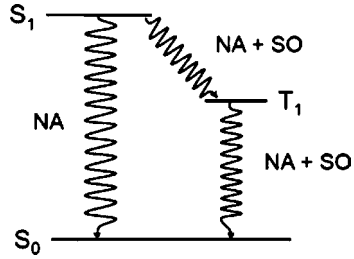

Figure 1. Jablonski diagram showing the nonradiative relaxation processes under investigation. The singlet excited state (S_1) decays to the ground state (S_0) by NA coupling. Alternatively, S_1 undergoes ISC to the lowest triplet state (T_1) by a combination of NA and SO couplings, and then another ISC takes T_1 to S_0.

Received: June 19, 2012
Published: September 11, 2012

   dx.doi.org/10.1021/ja305685v | *J. Am. Chem. Soc.* 2012, 134, 15648−15651

implementation[7,8,28] of the fewest-switches surface hopping (FSSH) technique for simulating coupled electron−phonon dynamics[29] within time-dependent Kohn−Sham (TDKS) theory.[30] The current work represents a major advance of the earlier theory because it includes spin−orbit (SO) coupling. Recent theoretical calculations and experimental investigations have shown[5,31,32] that SO coupling is strong in curved carbon nanostructures and that it can promote transfer of electronic excitation between different spin manifolds. Our simulations predict that S_1 decays to T_1 within tens of picoseconds, in agreement with the experimental result.[5] The magnitudes of the nonadiabatic (NA) electron−phonon and SO electronic couplings are similar; however, the NA coupling fluctuates more than the SO coupling. The fluctuation of the NA coupling is general to both the singlet and triplet manifolds. Nonradiative relaxation within the singlet manifold is accelerated when the NA coupling peaks.[7] Even though the ISC rate depends simultaneously on the magnitudes of the NA electron−phonon interaction and the SO interaction, our study indicates that it is determined primarily by the latter. The nonperturbative simulation showed that the ISC rate is proportional to the square of the SO coupling, validating a perturbation theory assessment such as the use of Fermi's golden rule. The electronic energy lost during ISC is deposited into high-frequency optical phonons produced by C−C stretching motions. The calculated homogeneous optical line widths of the singlet−triplet transitions are on the order of 10 meV at room temperature. This value is similar to the measured[14,33] and calculated[7] line widths of luminescence occurring within the singlet manifold. The predicted participation of the C−C stretching modes in ISC and the phosphorescence line width value can be measured spectroscopically in the future. The reported results indicate that ISC plays an important part in the nonradiative energy losses and low PL yields seen in the experiments.[14−16]

FSSH[29] is a technique for evolving a quantum-mechanical (electronic) subsystem coupled to classical-mechanical atomic motion. Reminiscent of quantum master equations, it defines instantaneous state-to-state transition rates that depend on the atomic evolution. In contrast to many other quantum−classical schemes, FSSH to a good approximation obeys detailed balance between transitions up and down in energy and leads to thermal equilibrium in the long-time limit. Therefore, it can be used to study relaxation processes. The implementation of FSSH within TDKS electronic structure theory[30]is described in ref 28, and ref 8 reports the application of FSSH-TDKS to the ultrafast relaxation of high-energy excitations in CNTs. The implementation of a semiclassical correction for decoherence/dephasing within FSSH-TDKS for the study of PL quenching in CNTs by nonradiative relaxation from S_1 to S_0 is described in ref 7.

The present study focused on ISC that occurs by a combination of SO coupling, which allows transitions between singlets and triplets, and NA coupling, which is responsible for transfer of the electronic energy released during a singlet−triplet transition to phonons. For this purpose, FSSH-TDKS was advanced to incorporate SO interactions,[34] as detailed in the Supporting Information (SI). The SO coupling induces transitions between different spin states. The S_0 and T_1 energies were computed with DFT as the ground-state energies for the singlet and triplet spin symmetries. The NA coupling was computed in the KS basis.[7,8,28] The SO coupling was obtained by performing the DFT calculations with and without the SO coupling interactions at every time step along the trajectory; the SO coupling was evaluated as half the difference of the singlet−triplet splittings obtained from the two calculations. Additional calculations were performed using the constant SO coupling values reported in the literature.[31]

The ISC study focused on the semiconducting (6,4) CNT, which has a significantly smaller unit cell than the (6,5) CNT studied experimentally.[5] A variety of S_1-T_1 energy splittings have been reported in the literature,[25−27] and we tested a range of possibilities. In our dynamics calculations, T_1 was 1 eV above S_0. The average SO coupling between T_1 and S_0 in our trajectory calculations was 1.6 meV. This is slightly smaller than the value of 2.4 meV produced in another theoretical study.[31] To test the importance of the magnitude of the SO coupling, we performed the calculations using each of these values. Since the SO coupling is predicted to be inversely proportional to the CNT diameter,[31,32] we also used the value of 1.0 meV to evaluate the ISC in larger-diameter CNTs.

The phonon-induced pure-dephasing/decoherence times for the S_1-T_1 and T_1-S_0 transitions were evaluated by computing the dephasing function $D(t)$, given by[35]

$$D(t) = \exp\left[\frac{\mathrm{i}}{\hbar}\langle \Delta E\rangle_{\mathrm{T}} t\right]\left\langle \exp\left\{-\frac{\mathrm{i}}{\hbar}\int_0^t \Delta E(\tau)\,\mathrm{d}\tau\right\}\right\rangle_{\mathrm{T}} \quad (1)$$

where ΔE is the energy difference between the states of interest and the angle brackets denote thermal averaging. The dephasing functions are shown in Figure 2. The data were fit

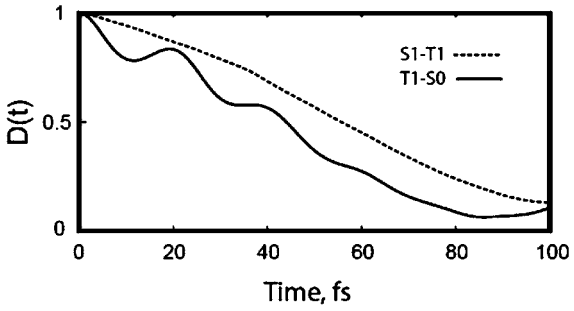

Figure 2. Dephasing functions (eq 1) describing phonon-induced pure dephasing of the S_1-T_1 and T_1-S_0 transitions. The dephasing times of 66 and 49 fs, respectively, correspond to values of 10 and 13 meV for the line widths, which can be measured.[14,33,36].

to an exponential, which was multiplied by a cosine in the T_1-S_0 case to capture the oscillatory part (see the SI). The pure-dephasing time calculated for the S_1-T_1 transition was $\tau_2^* = 66$ fs, while the T_1-S_0 dephasing was faster ($\tau_2^* = 49$ fs). The same approach produced a pure-dephasing time of 60 fs for the S_1-S_0 transition,[35] in agreement with the experimental data.[36] Dephasing occurs because of fluctuations of the electronic energy levels induced by vibrational motions. The SO coupling has little effect on the dephasing because it is small and nearly constant (see Figure 3a). The oscillation seen in the T_1-S_0 dephasing function shown in Figure 2 is caused by the optical G mode arising from C−C stretching motions. Radial breathing modes (RBMs) are responsible for the small-amplitude oscillations at longer times in Figure 2. RBMs contribute much more significantly to dephasing in CNTs with defects because defect sites are strongly coupled to RBMs.[35]

The pure-dephasing times are significantly shorter than the lifetimes determined below. Therefore, in the absence of

dx.doi.org/10.1021/ja305685v | J. Am. Chem. Soc. 2012, 134, 15648−15651

inhomogeneous broadening, which can be eliminated by photon-echo or single-molecule experiments, the width of the corresponding optical line (Γ) may be expressed as[35]

$$\Gamma = \frac{1}{\tau_2} = \frac{1}{2\tau_1} + \frac{1}{\tau_2^*} \approx \frac{1}{\tau_2^*} \quad (2)$$

where τ_2 is the overall dephasing time, τ_2^* is the pure-dephasing time, and τ_1 is the lifetime ($\tau_1 \gg \tau_2^*$). The homogeneous width of the T_1-S_0 line is 13 meV (Table 1), which is slightly larger than the S_1-S_0 width of 11 meV.[35] The phosphorescence line width can be detected in optical experiments.[14,33,36] If needed, the phosphorescence intensity can be increased, for instance, by atomic hydrogen absorption[37] and chemical functionalization,[38] following the strategy used to brighten the dark lowest-energy singlet exciton. [The calculated singlet-state optical absorption spectrum of the (6,4) CNT is shown in the SI].

Table 1. Singlet−Triplet Pure-Dephasing Times (τ_2^*), Fluorescence Line Widths (Γ), and ISC Times (τ_{ISC}) for the (6,4) CNT

transition	ΔE (eV)	τ_2^* (fs)	Γ (meV)	τ_{ISC} (ps)[a]
S_1-T_1	0.35	66	9	362/139/62.2
	0.10			97.3/39.7/16.7
T_1-S_0	1.05	49	13	1082/430/189
	1.30			1392/548/238

[a]At SO couplings of 1.0/1.6/2.4 meV.

Figure 3a shows the evolution of the NA and SO couplings over a representative 100 fs period. Their magnitudes are similar, but the SO coupling is much less sensitive to the atomic motion than the NA coupling. The fluctuation of the NA coupling with time is a general effect. The peaks in the NA coupling accelerate the nonradiative transition between the S_1 and S_0 states.[7] Similar to the case of the S_1-S_0 nonradiative relaxation, the energy lost during ISC is accommodated primarily by the high-frequency C−C stretching motions.

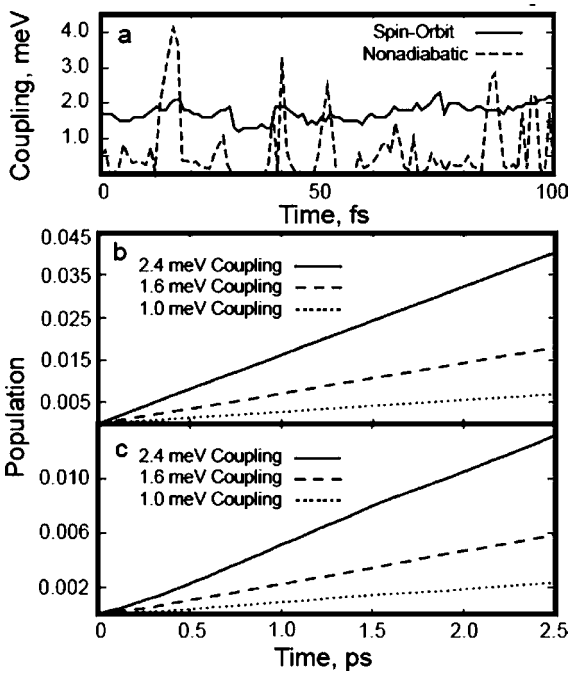

Figure 3. (a) Comparison of the magnitudes of the NA and SO couplings for the T_1-S_0 transition over a 100 fs trajectory window. (b, c) Evolution of the final state populations for the S_1-T_1 and T_1-S_0 transitions, respectively, corresponding to the 0.35 and 1.05 eV energy gaps (see Table 1).

Figure 3b,c presents the simulation results for the S_1-T_1 and T_1-S_0 ISC processes, respectively, obtained using different SO coupling values, including the one calculated in the present work (~1.6 meV; Figure 3a), the literature value (2.4 meV),[31] and the order of magnitude (1.0 meV). If it is assumed that the decay is exponential, as in the experiments,[5,9−11,14,15] the initial portion of the population versus time curve obtained in the simulation can be fit to $P(t) = 1 - \exp(t/\tau_{ISC}) \approx t/\tau_{ISC}$, producing the ISC times (τ_{ISC}) reported in Table 1. τ_{ISC} is inversely proportional to the square of the SO coupling, as predicted by perturbation theory (e.g., Fermi's golden rule). Thus, our nonperturbative simulation validates a perturbative treatment.

The S_1-T_1 transition occurs in tens to hundreds of picoseconds, depending on the strength of the SO coupling and the S_1-T_1 energy gap (Table 1). A larger energy gap, in agreement with ref 26, results in a slower transition. Reducing the gap according to the estimates from refs 25 and 27 speeds up the ISC. These time scales agree with the recent experimental data.[5] The S_1-S_0 transfer time evaluated previously for the (6,4) CNT is 150 ps, indicating that the S_1-T_1 ISC can compete with direct S_1-S_0 nonradiative relaxation. Theoretical studies of CNTs that included mixing between singlet and triplet manifolds predicted radiative lifetimes of 30−40 ns.[13] Therefore, the long-lived T_1 state[5] should emit light, enhancing the luminescence quantum yield.

The nonradiative decay of T_1 to S_0 was found by our calculations to occur within hundreds of picoseconds, depending on the SO coupling strength and the T_1-S_0 energy gap (Table 1). At low SO coupling, the T_1 lifetime exceeded 1 ns. Shifting the T_1-S_0 energy difference from 1.05 to 1.30 eV increased the triplet lifetime by ~20%. The experimental value for the T_1 excited state lifetime of the (6,5) CNT extends into microseconds.[5] This discrepancy could be resolved by reducing the T_1-S_0 SO coupling strength by 2 orders of magnitude. It should be noted that the SO coupling decreases with increasing CNT diameter, nearly vanishing for graphene.[39] At the same time, reducing the SO coupling for the S_1-T_1 transition strongly increases the S_1-T_1 transition time. One could potentially reconcile the theoretical and experimental results for the S_1-T_1 and T_1-S_0 transitions simultaneously by both reducing the SO coupling and either decreasing the S_1-T_1 energy gap or introducing higher-lying triplet states that are close in energy to S_1.

Our results suggest that phonon-assisted ISC can be an important nonradiative decay channel in CNTs. SO coupling in traditional carbon systems is weak. For instance, it has been predicted to be vanishingly small in graphene.[39] In contrast, efficient ISC mechanisms lead to a near-unity transfer of excited singlet states to long-lived triplet states in C_{60},[40] with an experimental rate constant of 5×10^8 s^{-1}. Since theoretical calculations have predicted that the SO coupling in small-diameter CNTs is as great as or greater than that in fullerenes,[31] it is not surprising that conversion from singlets to triplets may be efficient in CNTs. Our study considered only the transitions between the lowest singlet states and the lowest triplet state, excluding the full triplet state manifold. The inclusion of additional triplet states should increase the overall ISC rate.

dx.doi.org/10.1021/ja305685v | J. Am. Chem. Soc. 2012, 134, 15648−15651

Embedding the CNT in a matrix and providing other interactions with the environment would provide additional phonon modes to induce NA coupling and facilitate the relaxation. A matrix can distort the CNT, increasing its curvature and thus the SO coupling. Similarly, defects increase the local curvature and therefore the SO coupling, and they also create stronger NA coupling because of the more localized nature of excitations and phonon modes associated with defects. Thus, a host material and defects should accelerate ISC.

In conclusion, we have performed the first ab initio time-domain simulation of ISC in a CNT and calculated the phosphorescence line width. The calculated S_1-T_1 ISC time agrees with the recent experimental data,[5] and the line width can be measured in future experiments and compared with our prediction. We have identified the phonon modes that accommodate the electronic energy lost during ISC and shown that the electron−phonon and SO interactions have the same order of magnitude. Our results suggest that the S_1-T_1 ISC can provide an efficient nonradiative relaxation pathway in small-diameter CNTs. The rate of ISC can diminish in larger-diameter nanotubes as a result of the decrease in the SO coupling with increasing diameter and the dependence of the ISC rate on the square of the SO coupling. The S_1-T_1 ISC should definitely be considered when investigating the origin of the small yields of luminescence observed experimentally, even for larger-diameter nanotubes.

■ ASSOCIATED CONTENT

Supporting Information

Further calculation details, including a description of incorporating SO interactions into the FSSH-TDKS theory, fitting of the pure-dephasing functions shown in Figure 2, and an optical absorption spectrum of the (6,4) CNT at room temperature. This material is available free of charge via the Internet at http://pubs.acs.org.

■ AUTHOR INFORMATION

Corresponding Author

prezhdo@chem.rochester.edu

Notes

The authors declare no competing financial interest.

■ ACKNOWLEDGMENTS

The authors acknowledge NSF support through Grant CHE-1050405.

■ REFERENCES

(1) Dresselhaus, M. S.; Dresselhaus, G.; Saito, R.; Jorio, A. *Annu. Rev. Phys. Chem.* **2007**, *58*, 719.
(2) Carlson, L. J.; Krauss, T. D. *Acc. Chem. Res.* **2008**, *41*, 235.
(3) Wang, F.; Dukovic, G.; Brus, L. E.; Heinz, T. F. *Science* **2005**, *308*, 838.
(4) Scholes, G. D.; Rumbles, G. *Nat. Mater.* **2006**, *5*, 683.
(5) Park, J.; Deria, P.; Therien, M. J. *J. Am. Chem. Soc.* **2011**, *133*, 17156.
(6) Perebeinos, V.; Avouris, P. *Phys. Rev. Lett.* **2008**, *101*, No. 057401.
(7) Habenicht, B. F.; Prezhdo, O. V. *Phys. Rev. Lett.* **2008**, *100*, No. 197402.
(8) Habenicht, B. F.; Craig, C. F.; Prezhdo, O. V. *Phys. Rev. Lett.* **2006**, *96*, No. 187401.
(9) Huang, L.; Pedrosa, H. N.; Krauss, T. D. *Phys. Rev. Lett.* **2004**, *93*, No. 017403.
(10) Zhu, Z.; Crochet, J.; Arnold, M. S.; Hersam, M. C.; Ulbricht, H.; Resasco, D.; Hertel, T. *J. Phys. Chem. C* **2007**, *111*, 3831.
(11) Jones, M.; Metzger, W. K.; McDonald, T. J.; Engtrakul, C.; Ellingson, R. J.; Rumbles, G.; Heben, M. J. *Nano Lett.* **2007**, *7*, 300.
(12) Spataru, C. D.; Ismail-Beigi, S.; Capaz, R. B.; Louie, S. G. *Phys. Rev. Lett.* **2005**, *95*, No. 247402.
(13) Perebeinos, V.; Tersoff, J.; Avouris, P. *Nano Lett.* **2005**, *5*, 2495.
(14) Hagen, A.; Steiner, M.; Raschke, M. B.; Lienau, C.; Hertel, T.; Qian, H.; Meixner, A. J.; Hartschuh, A. *Phys. Rev. Lett.* **2005**, *95*, No. 197401.
(15) Jones, M.; Engtrakul, C.; Metzger, W. K.; Ellingson, R. J.; Nozik, A. J.; Heben, M. J.; Rumbles, G. *Phys. Rev. B* **2005**, *71*, No. 115426.
(16) Lefebvre, J.; Austing, D. G.; Bond, J.; Finnie, P. *Nano Lett.* **2006**, *6*, 1603.
(17) Ammu, S.; Dua, V.; Agnihotra, S. R.; Surwade, S. P.; Phulgirkar, A.; Patel, S.; Manohar, S. K. *J. Am. Chem. Soc.* **2012**, *134*, 4553.
(18) Zoberbier, T.; Chamberlain, T. W.; Biskupek, J.; Kuganathan, N.; Eyhusen, S.; Bichoutskaia, E.; Kaiser, U.; Khlobystov, A. N. *J. Am. Chem. Soc.* **2012**, *134*, 3073.
(19) Han, Z. J.; Ostrikov, K. *J. Am. Chem. Soc.* **2012**, *134*, 6018.
(20) D'Souza, F.; Das, S. K.; Zandler, M. E.; Sandanayaka, A. S. D.; Ito, O. *J. Am. Chem. Soc.* **2011**, *133*, 19922.
(21) Oelsner, C.; Antonia-Herrero, M.; Ehli, C.; Prato, M.; Guldi, D. M. *J. Am. Chem. Soc.* **2011**, *133*, 18696.
(22) Scholes, G. D.; Tretiak, S.; McDonald, T. J.; Metzger, W. K.; Engtrakul, C.; Rumbles, G.; Heben, M. J. *J. Phys. Chem. C* **2007**, *111*, 11139.
(23) Mohite, A. D.; Santos, T. S.; Moodera, J. S.; Alphenaar, B. W. *Nat. Nanotechnol.* **2009**, *4*, 425.
(24) Capaz, R. B.; Spataru, C. D.; Ismail-Beigi, S.; Louie, S. G. *Phys. Rev. B* **2006**, *74*, No. 121401.
(25) Capaz, R. B.; Spataru, C. D.; Ismail-Beigi, S.; Louie, S. G. *Phys. Status Solidi* **2007**, *244*, 4016.
(26) Tretiak, S. *Nano Lett.* **2007**, *7*, 2201.
(27) Aryanpour, K.; Mazumdar, S.; Zhao, H. *Phys. Rev. B* **2012**, *85*, No. 085438.
(28) Craig, C. F.; Duncan, W. R.; Prezhdo, O. V. *Phys. Rev. Lett.* **2005**, *95*, No. 163001.
(29) Tully, J. C. *J. Chem. Phys.* **1990**, *93*, 1061.
(30) Petersilka, M.; Gossmann, U. J.; Gross, E. K. U. *Phys. Rev. Lett.* **1996**, *76*, 1212.
(31) Huertas-Hernando, D.; Guinea, F.; Brataas, A. *Phys. Rev. B* **2006**, *74*, No. 155426.
(32) Keummeth, F.; Ilani, S.; Ralph, D. C.; McEuen, P. L. *Nature* **2008**, *452*, 448.
(33) Htoon, H.; O'Connell, M. J.; Cox, P. J.; Doorn, S. K.; Klimov, V. I. *Phys. Rev. Lett.* **2004**, *93*, No. 027401.
(34) Maiti, B.; Schatz, G. C. *J. Chem. Phys.* **2003**, *119*, 12360.
(35) Habenicht, B. F.; Kamisaka, H.; Yamashita, K.; Prezhdo, O. V. *Nano Lett.* **2007**, *7*, 3260.
(36) Graham, M. W.; Ma, Y.-Z.; Fleming, G. R. *Nano Lett.* **2008**, *8*, 3936.
(37) Nagatsu, K.; Chiashi, S.; Konabe, S.; Homma, Y. *Phys. Rev. Lett.* **2010**, *105*, No. 157403.
(38) Kilina, S.; Ramirez, J.; Tretiak, S. *Nano Lett.* **2012**, *12*, 2306.
(39) Boettger, J. C.; Trickey, S. B. *Phys. Rev. B* **2007**, *75*, No. 121402.
(40) Guldi, D. M.; Prato, M. *Acc. Chem. Res.* **2000**, *33*, 695.